

Fast counter-diabatic Thouless pumping in the Rice-Mele model

Joshua Chiel,¹ Christopher Jarzynski,^{1,2,3} and Jay Sau⁴

¹*Department of Physics, University of Maryland,
College Park, Maryland 20742-4111, US*

²*Department of Chemistry and Biochemistry,
University of Maryland, College Park, MD 20742 USA*

³*Institute for Physical Science and Technology,
University of Maryland, College Park, MD 20742 USA*

⁴*Joint Quantum Institute and Condensed Matter Theory Center,
Department of Physics, University of Maryland,
College Park, Maryland 20742-4111, US*

(Dated: March 18, 2024)

Abstract

Thouless pumping is a transport phenomenon where a periodically varying Hamiltonian can transfer a quantized amount of charge when the time-dependence of the Hamiltonian is quasi-adiabatic. Past proposals to speed up this process involving Floquet techniques lead to a subtle problem of setting the initial state of the system. In this work we apply counter-diabatic driving to the Rice-Mele model, which is one of the simplest models for Thouless pumping, to ensure that the system remains in the ground state for any driving speed. We show that the pumped charge across each bond of the Rice-Mele model is given by a topologically quantized Chern number in this case. However, the counter-diabatic driving in a general case turns out to involve long-range hopping. We show that this can be mitigated either by choosing a very specific example of the Rice-Mele model or by numerical optimization of the Hamiltonian to create experimentally realizable variants of fast pumping in the Rice-Mele model.

I. INTRODUCTION

Topological Thouless pumps provide dissipationless transport that is robustly and exactly quantized [1]. A Thouless pump is driven by a time-periodic Hamiltonian, and the charge that is pumped per driving cycle is given by a Chern number associated with the system's ground state. In its original formulation, a Thouless pump must be driven adiabatically, i.e. slowly relative to the time scale set by the ground state gap. It is natural to ask whether the same result – quantized, dissipationless transport – can be achieved without the requirement of slow driving.

A growing field of study addresses this question. One approach is to take advantage of the time-periodicity of the Hamiltonian in the Thouless scheme and view it as a Floquet Hamiltonian. In this case, it was shown that states in a gapped Floquet band can exhibit quantized charge pumping [2]. Similar fast pumping can occur in the anomalous Floquet-Anderson insulator [3]. However, these cases require fine-tuning of initial conditions to occupy quasi-energy bands, which generally differ from the ground state of the Hamiltonian. Explicitly including damping can also lead to fast pumping in open dissipative systems [4] governed by a non-Hermitian generalization of the Rice-Mele Hamiltonian. Both the Floquet Hamiltonian approach and the open system setting differ from the case considered originally by Thouless,

in which a closed quantum system begins in the ground state of a static Hamiltonian, then undergoes quantized pumping during one cycle of driving, and finally returns to the ground state.

Shortcuts to adiabaticity (STA) offer a natural, additional line of attack to speed up transport and preserve a given state (in this case the ground state) of a system throughout the system’s evolution [5]. In the counterdiabatic (CD) approach, given a time-dependent Hamiltonian $H_0(t)$ and a system initialized in an arbitrary instantaneous eigenstate of $H_0(t)$, adding an appropriately designed auxiliary term $H_{CD}(t)$ causes the system to remain in this eigenstate of $H_0(t)$ at all times. That is, the CD Hamiltonian $H_{CD}(t)$ suppresses transitions to other eigenstates [6–8]. CD methods have also been employed to speed up classical geometric pumps [9, 10] and have been applied to a Cooper-pair pump, which is a bosonic system with an effectively single phase quantum degree of freedom [11].

In this work, we apply CD methods to the standard Thouless pump i.e. a non-interacting fermionic chain in one dimension where the pumping protocol starts in the ground state of an initial Hamiltonian. The system then evolves under the Hamiltonian $H_0(t) + H_{CD}(t)$ as $H_0(t)$ varies periodically in time for a finite number of periods. By adding H_{CD} to H_0 we preserve the filled single particle Bloch states of H_0 throughout the system’s evolution. We will show that for any gapped “original” Hamiltonian $H_0(t)$, the charge pumped across each bond of the system (see Fig. 1) is given by a Chern number of the ground state density matrix of $H_0(t)$ and is therefore quantized in a topologically robust way. While CD driving can produce fast quantized particle transport arbitrarily fast, for an appropriate choice of $H_{CD}(t)$, the resulting H_{CD} can potentially have arbitrarily long-range hopping terms, that limits its experimental realizability. We show that this problem can be avoided using the so-called “control-freak” protocol [12] of the Rice-Mele (RM) model [13] shown in Fig. 1. This protocol provides a specific, though fine-tuned, example of $H_0(t)$ where $H_{CD}(t)$ contains only nearest neighbor hopping terms and is therefore realizable. We show that the charge pumping in this protocol is given by a quantized Chern number. For the case of more general Hamiltonians $H_0(t)$, we find an approximate solution to H_{CD} which involves only nearest neighbor hopping using a numerical optimization procedure.

This paper is structured as follows. In section II we review the Rice-Mele model and derive an exact CD protocol for it. In section III we construct a current density operator

and show that the exact CD protocol preserves the pumped charge over a cycle. In section IV we develop a general approach to construct nearest neighbor Hamiltonians that will produce finite-time Thouless pumping, and we conclude in section V by discussing our results.

II. CD RICE-MELE MODEL

The Rice-Mele model provides a useful lattice model of non-interacting Thouless pumping. When driven through a quasi-adiabatic cycle, the system produces quantized particle transport. The model consists of a 1d chain of atoms, two per unit cell, with two types of bonds – intracell bonds and intercell bonds. See Figure 1. In real space we have:

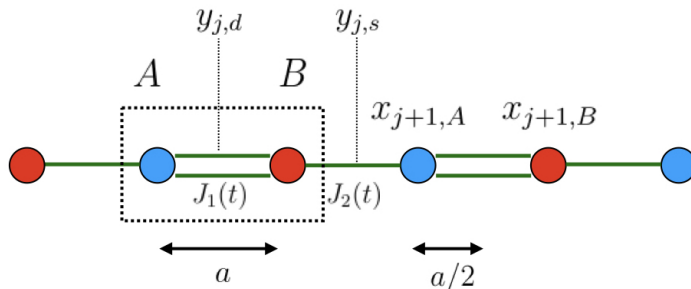


FIG. 1: The Rice-Mele 1d lattice model consists of a 1d chain of two types of atoms, with positions $x_{j,A} = aj$ (blue) and $x_{j,B} = a(j + 1)$ (red), connected by intracell bonds (d, double green lines) at positions $y_{j,d} = a(j + 1/2)$ and intercell bonds (s, single green lines) at positions $y_{j,s} = a(j - 1/2)$. The dashed box shows a unit cell. The intracell/intercell hopping amplitudes are given by $J_{1/2}$.

$$\hat{H}_0(t) = - \sum_j \left(J_1(t) \hat{a}_j^\dagger \hat{b}_j + J_2(t) \hat{a}_{j+1} \hat{b}_j + h.c. \right) + \Delta(t) \sum_j \left(\hat{a}_j^\dagger \hat{a}_j - \hat{b}_j^\dagger \hat{b}_j \right) \quad (1)$$

where $\hat{a}_j^\dagger(\hat{a}_j)$ and $\hat{b}_j^\dagger(\hat{b}_j)$ are the creation (annihilation) operators acting on the left and right sites of the j th unit cell. In the position representation, the two locations of physical atoms per unit cell are $x_{j,A} = aj$ and $x_{j,B} = a(j + 1)$. We also write the locations of the intracell bonds as $y_{j,d} = a(j + 1/2)$ and the intercell bonds as $y_{j,s} = a(j - 1/2)$. The time dependent coefficients $J_1(t)$, $J_2(t)$ and $\Delta(t)$ tune the intracell hopping amplitude, intercell hopping amplitude, and a staggered on-site potential respectively. In momentum space, the

Hamiltonian can be written as

$$\hat{H}_0(k, t) = \mathbf{R}(k, t) \cdot \boldsymbol{\sigma}, \quad (2)$$

where $\boldsymbol{\sigma}$ are 2×2 Pauli matrices acting on the space of Bloch states $(\tilde{a}_k^\dagger, \tilde{b}_k^\dagger)^T$ with $\tilde{a}_k^\dagger, \tilde{b}_k^\dagger$ being Fourier transforms of the orbital operators a_j^\dagger and b_j^\dagger respectively and

$$\mathbf{R}(k, t) = \{-J_1(t) - J_2(t) \cos(ka), -J_2(t) \sin(ka), \Delta(t)\}, \quad (3)$$

where $J_{1/2}(t)$ and $\Delta(t)$ are periodic on the interval $[0, T]$. We moreover assume that $R(k, t)$ is constant outside of $(0, T)$. We note that this gives us a Floquet-Bloch Hamiltonian, which is gapped for all k, t away from $J_1(t) - J_2(t) = \Delta(t) = 0$. We emphasize that our system will thus begin and end in the ground state of H_0 , rather than requiring an initialization into a particular Floquet-Bloch state in the infinite past.

Eq. (2) has the same form as that considered by Berry[8] (see Eq. 3.1 therein). Since this is a two-band system, we can immediately evoke Berry's results and write down the corresponding $H_{CD}(k, t)$ in lattice-momentum space:

$$\hat{H}(k, t) = \hat{H}_0(k, t) + \hat{H}_{CD}(k, t) = \left(\mathbf{R} + \frac{1}{R^2} \mathbf{R} \times \partial_t \mathbf{R} \right) \cdot \boldsymbol{\sigma} \equiv \mathbf{u} \cdot \boldsymbol{\sigma}. \quad (4)$$

where we define $\mathbf{u}(k, t)$, a vector which is periodic in k and t . For a system initialized in its single particle ground Bloch state of H_0 , we will show that in the presence of H_{CD} , the particle transport remains quantized under arbitrarily fast driving. Note that \hat{H}_{CD} is manifestly periodic and smooth in k and thus, by a well known theorem of Fourier analysis, \hat{H}_{CD} is exponentially localized in real space.

III. PUMPED CHARGE

Even granting the spatial, exponential-locality of \hat{H}_{CD} , it is not *a priori* obvious how to define a current operator for an operator whose matrix elements involve two distinct spatial points. We will employ a generalized Peierls substitution method to define such a current and show it gives the desired result.

We consider an arbitrary non-local Hamiltonian in one spatial dimension:

$$i\partial_t\Psi(x) = \sum_{x'} H(x, x')\Psi(x') \quad (5)$$

where $x, x' \in \{aj : j \in \mathbb{Z}\}$ represent positions of atoms/sites. Motivated by the Peierls substitution method [14] framework, we introduce a vector potential $A(y)$ on the bonds as follows:

$$H(x, x')[A] = H(x, x')e^{i\text{sign}(x-x')\sum_{x<y<x'} A(y)} \quad (6)$$

where $H(x, x')$ is the non-local Hamiltonian introduced above, and y live on bonds, i.e. $y_{s/d} \in \{a(j/2 \pm 1) : j \in \mathbb{Z}\}$. The current operator in the tight-binding approximation can be written as:

$$\langle x | \hat{J}(y) | x' \rangle = \left. \frac{\delta H(x, x')[A]}{\delta A(y)} \right|_{A \rightarrow 0} = i \left(\Theta(y - x) - \Theta(y - x') \right) H(x, x') \quad (7)$$

where Θ is the Heaviside step function. Note that, consistent with Fig. 1, we label the position of the bonds with y , which is where the vector potential connects sites x, x' . In appendix A we show this current density operator satisfies a continuity equation.

The total current operator of the system (with periodic boundary conditions) $\hat{j} = a \sum_y \hat{J}(y)$ can be computed from the local current density calculated in Eq. 7 as:

$$\langle x | \hat{j} | x' \rangle = ia \sum_y \left(\Theta(y - x) - \Theta(y - x') \right) H(x, x') = i(x - x')H(x, x') \quad (8)$$

for any pair of points x, x' away from the boundary $x = 0, L$, which matches the expression for average current in the crystal [15]. Using lattice translational invariance, the total current over a unit-cell is written as

$$\begin{aligned} j_{cell}(t) &= \sum_{R, x'} \langle x | \hat{j} | x' + R \rangle \rho(x' + R, x) \\ &= \sum_{R, x'} i(x - x' + R)H(x, x' + R)\rho(x' + R, x) \end{aligned} \quad (9)$$

where $\rho(x, x' + R)$ is the density matrix of the occupied states. Writing the real space

Hamiltonian in terms of the Bloch Hamiltonian $H(x, x' + R) = \int \frac{dk}{2\pi} e^{ik(x-x'+R)} H_k(x, x')$ as well as the density matrix in the above equation and then using $H(k, t)$ in Eq. (4) for the Bloch Hamiltonian together with $\hat{\rho}_k(t) = \frac{1}{2} (\sigma_0 - \hat{\mathbf{R}}(k, t) \cdot \boldsymbol{\sigma})$ as the density matrix, the average current in the system simplifies to:

$$j_{cell}(t) = \int \frac{dk}{2\pi} Tr[\partial_k H(k, t) \rho_k^\dagger] = \int \frac{dk}{2\pi} \partial_k \mathbf{u} \cdot \hat{\mathbf{R}}, \quad (10)$$

where $\hat{\mathbf{R}} = \mathbf{R}/R$.

The current $j_{cell}(t)$ is actually the total current over all bonds in the unit-cell. The physical charge pumped across a unit-cell is the average over the unit-cell in terms of bonds i.e.

$$Q_{pump}(t) = \int_0^t d\tau j_{cell}(\tau) / N_{cell}, \quad (11)$$

where N_{cell} is the number of sites in the unit-cell. For the Rice-Mele model, $N_{cell} = 2$. Integrating (11) by parts, and substituting \mathbf{u} from Eq.(4) we find

$$Q_{pump}(t) = \frac{1}{4\pi} \int_0^t d\tau \int_{-\frac{\pi}{a}}^{\frac{\pi}{a}} dk \hat{\mathbf{R}} \cdot (\partial_k \hat{\mathbf{R}} \times \partial_t \hat{\mathbf{R}}). \quad (12)$$

It is manifest from the final line of Eq. 12 that the pumped charge at the end of the cycle $Q_{pump}(T)$ is the Chern number C of the vector field $\hat{\mathbf{R}}(k, t)$ over the torus and is an integer as long as $\hat{\mathbf{R}}(k, t)$ is a continuous vector field on the torus due to $\hat{\mathbf{R}}$'s periodic boundary conditions in k and t [16].

Note that Eq. (8) matches the standard current operator form[15] which is for the average current over a unit cell. In the quasi-adiabatic regime, charge does not build up in the cell, so average current is the only relevant quantity. Indeed, $Q_{pump}(t)$ is the charge pumped across the unit-cell and does not represent the complete motion of the charge across bonds. This information is provided by the time-dependent density of charge in the unit-cell

$$Q(x, t) = \int_{-\pi/a}^{\pi/a} \frac{dk}{2\pi} \rho_k(x, x) = \int \frac{dk}{2\pi} (1 - \hat{R}_z(k, t) s_{\sigma(x)}) \quad (13)$$

where \hat{R}_z is the z th component of $\hat{\mathbf{R}}$. For a given cell, we take the atom sites to be at

$x \in \{0, a\}$ and bond positions to be $x_b \in \{-a/2, a/2\}$ and so $s_\sigma(0) = -1$ and $s_\sigma(a) = 1$. The charge pumped across any bond b , is $Q_{pump,b}(t) = \int d\tau \langle x | J(y_b) | x' \rangle$, where $J(y_b) = Tr(\hat{\rho} \hat{J})$ is the expectation value of the current operator defined in Eq. (7). Using the conservation law $\partial_t Q(x, t) = a^{-1}(J(x + a/2) - J(x - a/2))$ together with Eq. (11), we find

$$Q_{pump,b}(t) = Q_{pump}(t) + \sum_{x \in \{0, a\}} \Phi(x, x_b)(Q(x, t) - Q(x, 0)), \quad (14)$$

which rearranges charge in the unit-cell in addition to pumping charge across the cell. Moreover, $\Phi(x, x_b) = \Theta(x - x_b) - x/a$ is determined from $a^{-1} \int dx_b Q_{pump,b} = Q_{pump}(t)$. The latter contribution vanishes in the adiabatic case since the density matrix retains the ground state form. Note that $Q_{pump,b}(T) = Q_{pump}(T)$.

IV. FINITE-TIME, NEAREST-NEIGHBOR THOULESS PUMPS

Equations (4) and (12) imply that a time-dependent, Bloch Hamiltonian $H(k, t) = H_0(k, t)$ in the quasi-adiabatic regime gives rise to a Thouless pump if and only if $H(k, t) = H_0(k, t) + H_{CD}(k, t)$ gives rise to a Thouless pump for arbitrary fast driving. Hence, for the purpose of demonstrating a “fast” Thouless pump, we can choose a form for $H(k, t)$ that is experimentally realizable, and reverse-engineer a corresponding $H_0(k, t)$, so long as H_0 is periodic in t and gapped for all k and t (H_0 is automatically periodic in k as a Bloch Hamiltonian). For the purposes of this work, “an experimentally realizable” protocol refers to a RM model with complex hopping terms i.e. can be described by Eq. (4) with

$$\mathbf{u}(k, t) = Re[\{-u_1(t) - u_2(t)e^{ika}, -iu_1(t) - iu_2(t)e^{i(ka)}, u_0(t)\}] \quad (15)$$

where the hopping parameters $J_{1,2}(t)$ in Fig. 1 are replaced by $u_{1,2}(t)$, which are now allowed to be complex. The total Hamiltonian H generated using Eq. 4 starting with H_0 given by an RM model is typically not a nearest neighbor model (i.e. does not satisfy the constraint above) and therefore experimentally challenging to implement. Therefore, we choose $\mathbf{u}(k, t)$ to satisfy the above constraint and solve for \mathbf{R} using Eq. 4 to determine $H_0(k, t)$, which is now not necessarily a RM model. Furthermore, the system must start in the ground state of the Hamiltonian $H(k, t < 0)$ and return to the ground state at the end of the protocol,

which leads to the constraint

$$\mathbf{R}(k, 0) = \mathbf{u}(k, t < 0) = \mathbf{u}(k, t > T) = \mathbf{R}(k, T). \quad (16)$$

This condition is critical to ensuring that \mathbf{R} is periodic in k and t during the drive, which in turn is required for the periodicity condition that leads to quantization of the pumped charge. While the first half of this condition is simply set as an initial condition for \mathbf{R} in Eq. 4 viewed as a time-evolution equation for $\mathbf{R}(k, t)$, the second half constrains the final value $\mathbf{R}(k, t)$ of the solution. As discussed below this constraint is satisfied by choosing $\mathbf{u}(k, t)$ according to Eq. (15).

To determine the appropriate $\mathbf{R}(k, t)$, we start by noting that the equation for $H_0(k, t)$ (i.e. Eq. (4)) is explicitly written as a differential equation $\mathbf{u} = \left(\mathbf{R} + \frac{1}{R^2}\mathbf{R} \times \partial_t \mathbf{R}\right)$. This equation can be simplified into a differential equation

$$\partial_t \hat{\mathbf{R}} = \mathbf{u} \times \hat{\mathbf{R}} \quad (17)$$

with the magnitude of \mathbf{R} determined by

$$R = \mathbf{u} \cdot \hat{\mathbf{R}}. \quad (18)$$

The above problem can be solved numerically to find solutions near a RM model with particular parameters. However, before that we discuss an analytically soluble limit that is based on Thouless pumping using the so-called "control freak" protocol [12]. This protocol was shown to allow quantized pumping at arbitrary speeds but is somewhat limited because it requires one of $J_{1,2}(t)$ in Fig. 1 to vanish at any instant of time, so that the lattice is never completely connected. At the same time, this limit provides a nice analytic limit to study pumping [12] and therefore we use this as an analytic test example. For such a limit, we use an ansatz for the vector

$$\begin{aligned} \mathbf{R}(k, 0 < t < T/2) &= (R_{\perp}(t), 0, R_{\parallel}(t)) \\ \mathbf{R}(k, T/2 < t < T) &= (R_{\perp}(t) \cos k, R_{\perp}(t) \sin k, R_{\parallel}(t)). \end{aligned} \quad (19)$$

This ansatz corresponding to the so-called “control freak” protocol [12] where the first phase $0 < t < T/2$ corresponds to a state where electrons are delocalized on one set of bonds and the second phase corresponds to electrons on the other set $T/2 < t < T$. The latter set of bonds are entirely inside the unit cell (i.e. double bonds in Fig. 1) and therefore lead to a Hamiltonian with no k -dependence. The total Hamiltonian to implement this protocol is given by a vector $\mathbf{u}(k, 0 < t < T/2) = \mathbf{R}(k, t) + \dot{\theta}(0, 1, 0)$ and $\mathbf{u}(k, T/2 < t < T) = \mathbf{R}(k, t) + \dot{\theta}(-\sin k, \cos k, 0)$, which clearly satisfies the constraint Eq. 15. Here we have reparameterized the time-dependence of $R_{\perp, \parallel}(t)$ as $R_{\parallel}(t) = e^{\lambda(t)} \cos \theta(t)$ and $R_{\perp}(t) = e^{\lambda(t)} \sin \theta(t)$. Continuity and time-periodicity of the vector $\mathbf{R}(k, t)$ require $\theta(t = 0) = 0$, $\theta(T/2) = \pi$ and $\theta(t = T) = 2\pi$. Substituting \mathbf{R} from Eq. 19 into the pumped charge Eq. 12 we get $Q_{pump}(T/2 < t < T) = \cos \theta(t)$ (and $Q_{pump}(0 < t < T/2) = 0$). Substituting into Eq. 13, $Q(0, 0, t) - Q(0, 0, 0) = (1 - \cos \theta(t))/2$. These can be combined, using Eq. 14, into equations for charge pumped across each bond:

$$\begin{aligned} Q_{pump,d}(0 < t < T/2) &= 0, & Q_{pump,d}(T/2 < t < T) &= \frac{(1 + \cos \theta(t))}{2} \\ Q_{pump,s}(0 < t < T/2) &= \frac{(1 - \cos \theta(t))}{2}, & Q_{pump,s}(T/2 < t < T) &= 1, \end{aligned} \quad (20)$$

where $\theta(t)$ varies from 0 to 2π over the protocol. Based on these boundary conditions for θ it is clear that both $Q_{pump,s}$ and $Q_{pump,d}$ increase from 0 to 1 over a time-period. Furthermore, a single electron is pumped across the d -bond in Fig. 1 from site A to B over the first half of the cycle followed by the electron being pumped across the s -bond from site B to A in the second half of the protocol.

In the case of a generic starting RM model, we numerically solve these differential equations for $\mathbf{R}(k, t)$ with the initial condition $\mathbf{R}(k, 0) = \mathbf{u}(k, t < 0)$ (i.e. Eq. 16). For these results we choose $J_{1/2} = J_0 \pm \delta_0 \cos(\varphi(t) + \phi_{shift})$ and $\Delta(t) = \Delta_0 \sin(\varphi(t) + \phi_{shift})$, with lattice spacing a and $\omega = 2\pi/T$, for some period T , so that $H_0(t)$ comes back to itself after a period T . Here ϕ_{shift} is a time shift to allow one to choose general initial starting points. The function $\varphi(t) = \pi(1 - \cos(\omega t/2))$ ensures that the derivative of $\partial_t \mathbf{R}(k, t)|_{t=0, T} = 0$. We then vary $\mathbf{u}(k, t)$ by choosing $u_j(t) = u_j^{(0)}(t) + \sum_{n \geq 0} (u_{j,n} e^{in\varphi(t)})$ where the coefficients $u_{j,n \neq 0}$ are chosen by numerical optimization (fminunc in MATLAB) to minimize the least squares error in the final condition i.e. $\mathcal{E} = \sum_k |\mathbf{R}(k, T) - \mathbf{R}(k, 0)|^2$ where the sum is taken over

a discrete grid of k . Here the functions $u_j^{(0)}(t)$ set the starting point of the iteration to the Rice-Mele vector vector $\mathbf{u}(k, t) = \mathbf{R}(k, t)$ in Eq. 3.

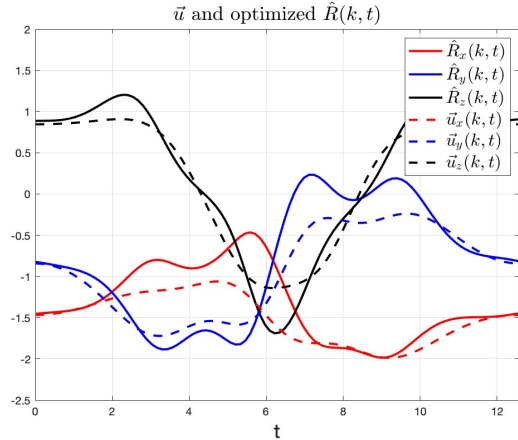
The components of the optimized solution $\hat{\mathbf{R}}(k, t)$ for the protocol are plotted in Figure 2 along with the components of \mathbf{u} , the input to the optimization method, for fixed $\omega = 0.5$ and $k = 1.1$. The parameters for the simulation are chosen to be $a = 1$, $J_0 = 1.1$, $\delta_0 = 0.9$, $\Delta_0 = 1$, with a uniform mesh of one hundred t points between $(0, T)$. Notice the approximate periodicity of \hat{R}_i and their being non-zero. We see from Figure that $\min_k (R(k, t)) > 0$ for all t , thus ensuring that the reverse-engineered $H_0(k, t)$ will be gapped for all k and t . The error metric \mathcal{E} sums over a uniform mesh of one hundred k points between $(-\pi/a, \pi/a)$.

From the plot of Q_{pump} and $Q_{pump,b}$ of Eq. (12) and Eq. (14) in Figure 3 a simple physical picture emerges: the particle at site A is sequentially pumped to site B in the same unit cell and then pumped to site A in the next unit cell. This follows from the pumped charge initially being larger across the bond linking A to B within the same unit cell to then flipping to be larger on the bond linking B to A on the next unit cell. This is qualitatively similar with the result for the ideal fast pumping model described by Eq. 20.

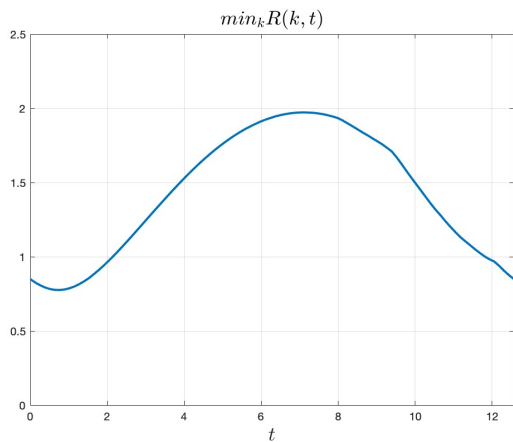
V. DISCUSSION

Starting from a Rice-Mele model, we derive an exact H_{CD} protocol and analytically show that it preserves the charge pumped across each bond in the model (see Fig. 1) as a Chern number. We do this by determining the pumped charge $Q_{pump,b}(t)$ for the two types of bond s and d in the lattice shown in the RM model shown in Fig. 1. However, this exact H_{CD} involves higher harmonics of k which in real space correspond to long-range hopping terms. Experimentally, such terms are challenging if not impossible to actualize. The total Hamiltonian $H = H_0 + H_{CD}$ is what is actually implemented in an experiment. Based on this we considered the possibility of restricting $H(t)$ to only include nearest neighbor hopping terms through Eq. 15.

With this constraint we found that the “control freak” protocol on the RM model [12] allowed for an analytically soluble example of fast pumping in an RM model as was clear from Eq. 20. We then relaxed the requirements by numerically finding a more general Hamiltonian $\mathbf{u}(t)$, which led to quantized charge pumping as was seen in Fig. 3. In both these case, the



(a)



(b)

FIG. 2: (a) The components of $\mathbf{u}(k, t)$ from Eq. (15) which are inputs to the numerical optimization method plotted with the components of $\hat{R}(k, t)$ which are the output of the method and solutions to (17) subject the boundary conditions described in the main text. Plots produced for $\omega = 0.5$ and $k = 1.1$. Notice the approximate periodicity of \hat{R}_i and their being non-zero. (b) $\min_k(R(k, t))$ calculated from the output of the optimization method as a function of t . Here again, $\omega = 0.5$. We see that the magnitude of $R(k, t)$ is greater than 0 for all t and k thus ensuring that the reverse-engineered $H_0(k, t) = \mathbf{R}(k, t) \cdot \boldsymbol{\sigma}$ will be gapped for all k and t .

time-dependence of the charge pumped across bonds provided a physical interpretation of the charge being first pumped from site A to B and then back to site A in the next unit-cell. These results on fast quantized pumping over a class of Hamiltonians provide a wealth of opportunities for experimental realizations of finite-time Thouless pumps.

The Rice-Mele model we considered is a lattice model, that in k space is a two-band system, without disorder or interactions. Applying STA methods to multiband lattice systems

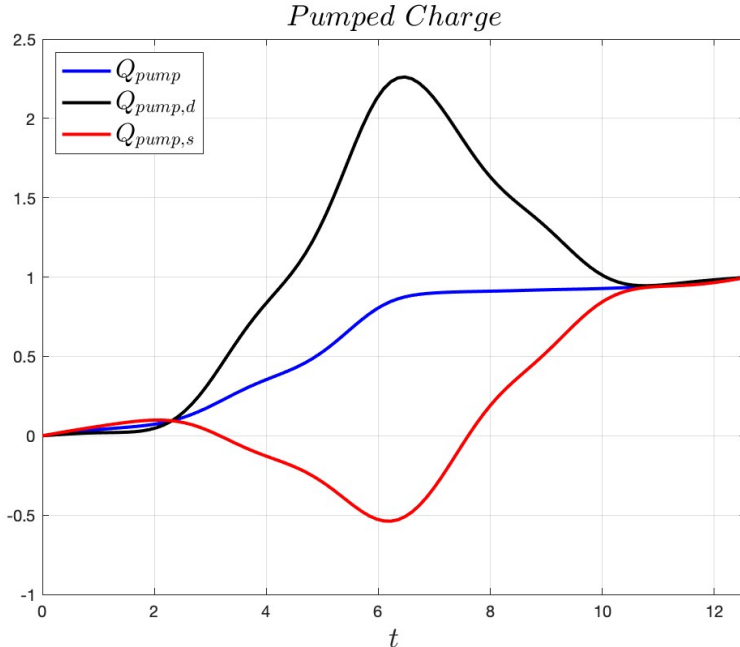


FIG. 3: $Q_{pump}(t)$ of Eq. (12) and $Q_{pump,b}$ of Eq. (12) for $\omega = 0.5$. Note the quantization of pumped charge over a cycle T . Physically, the particle at site A is sequentially pumped to site B in the same unit cell and then pumped to site A in the next unit cell.

and systems involving interactions and disorder are important future steps. Our work contributes to the promise of actualizing finite-time, robust and dissipationless charge transport.

Note added: In the process of completing this manuscript, we became aware of the preprint by Liu *et al* [17], who also apply counterdiabatic methods to the Rice-Mele model. Their work focuses on Wannier centers, and they obtain a counterdiabatic field \mathbf{u} that generally includes non-nearest-neighbor interactions.

Acknowledgements: JC is supported by the National Science Foundation Graduate Research Fellowship Program under Grant No. DGE 2236417. CJ acknowledges support by the U.S. National Science Foundation under Grant No. 2127900. Any opinions, findings, and conclusions or recommendations expressed in this material are those of the authors and do not necessarily reflect the views of the National Science Foundation. J.S. acknowledges support from the Joint Quantum Institute and support by the Laboratory for Physical Sciences through its continuous support of the Condensed Matter Theory Center at the University of Maryland. JC gratefully acknowledges Michael Hinczewski and Sebastian Deffner for helpful conversations.

Appendix A: Current density operator

Starting from (7), we consider the right hand side of the continuity equation. For this purpose we define a discrete derivative $\delta_x f(x) = f(x + a/2) - f(x - a/2)$, where the function f is defined over bond when x is on a site. The discrete analog of the continuity equation is then given by:

$$\begin{aligned}
-\delta_x \langle \hat{J} \rangle &= -\delta_x \left(\sum_{x_1, x'} \Psi^*(x_1) \langle x_1 | \hat{J}(x) | x' \rangle \Psi(x') \right) \\
&= -i \sum_{x_1, x'} \Psi^*(x_1) H(x_1, x') \Psi(x') (\delta_{x, x_1} - \delta_{x, x'}) \\
&= -i \left(\sum_{x'} \Psi^*(x) H(x, x') \Psi(x') - \sum_{x_1} \Psi^*(x_1) H(x_1, x) \Psi(x) \right) \\
&= -i \left(\sum_{x_1} \Psi^*(x) H(x, x_1) \Psi(x_1) - \sum_{x_1} (\Psi(x) (H(x, x_1))^* \Psi(x_1)) \right) \\
&= \Psi^*(x) \partial_t \Psi(x) + \Psi(x) \partial_t \Psi^*(x) \\
&= \partial_t \rho(x)
\end{aligned} \tag{A1}$$

Thus, the current density operator defined in (7) satisfies a continuity equation.

-
- [1] D. Thouless, Physical Review B **27**, 6083 (1983).
 - [2] T. Kitagawa, E. Berg, M. Rudner, and E. Demler, Physical Review B **82**, 235114 (2010).
 - [3] P. Titum, E. Berg, M. S. Rudner, G. Refael, and N. H. Lindner, Physical Review X **6**, 021013 (2016).
 - [4] Z. Fedorova, H. Qiu, S. Linden, and J. Kroha, Nature communications **11**, 3758 (2020).
 - [5] D. Guéry-Odelin, A. Ruschhaupt, A. Kiely, E. Torrontegui, S. Martínez-Garaot, and J. G. Muga, Reviews of Modern Physics **91**, 045001 (2019).
 - [6] M. Demirplak and S. A. Rice, The Journal of Physical Chemistry A **107**, 9937 (2003).
 - [7] M. Demirplak and S. A. Rice, The Journal of Physical Chemistry B **109**, 6838 (2005).
 - [8] M. V. Berry, Journal of Physics A: Mathematical and Theoretical **42**, 365303 (2009).
 - [9] K. Funo, N. Lambert, F. Nori, and C. Flindt, Physical Review Letters **124**, 150603 (2020).

- [10] K. Takahashi, K. Fujii, Y. Hino, and H. Hayakawa, *Physical Review Letters* **124**, 150602 (2020).
- [11] P. A. Erdman, F. Taddei, J. T. Peltonen, R. Fazio, and J. P. Pekola, *Physical Review B* **100**, 235428 (2019).
- [12] J. K. Asbóth, L. Oroszlány, and A. Pályi, *Lecture notes in physics* **919**, 166 (2016).
- [13] M. Rice and E. Mele, *Physical Review Letters* **49**, 1455 (1982).
- [14] X.-L. Qi and S.-C. Zhang, *Reviews of Modern Physics* **83**, 1057 (2011).
- [15] D. Vanderbilt, *Berry phases in electronic structure theory: electric polarization, orbital magnetization and topological insulators* (Cambridge University Press, 2018).
- [16] M. Z. Hasan and C. L. Kane, *Reviews of modern physics* **82**, 3045 (2010).
- [17] W. Liu, Y. Ke, and C. Lee, arXiv preprint arXiv:2401.17081 (2024).